Steel and Composite Structures, *Vol. 26, No. 1 (2018) 1-15*
DOI: https://doi.org/10.12989/scs.2018.26.1.001

Stochastic bending characteristics of finite element modeled Nano-composite plates

Shivaji G. Chavan* and Achchhe Lal[a]

Department of Mechanical Engineering, S.V. National Institute of Technology, Surat - 395007, India

(*Received March 13, 2017, Revised September 6, 2017, Accepted September 22, 2017*)

Abstract. This study reported, the effect of random variation in system properties on bending response of single wall carbon nanotube reinforced composite (SWCNTRC) plates subjected to transverse uniform loading is examined. System parameters such as the SWCNT armchair, material properties, plate thickness and volume fraction of SWCNT are modelled as basic random variables. The basic formulation is based on higher order shear deformation theory to model the system behaviour of the SWCNTRC composite plate. A C0 finite element method in conjunction with the first order perturbation technique procedure developed earlier by the authors for the plate subjected to lateral loading is employed to obtain the mean and variance of the transverse deflection of the plate. The performance of the stochastic SWCNTRC composite model is demonstrated through a comparison of mean transverse central deflection with those results available in the literature and standard deviation of the deflection with an independent First Order perturbation Technique (FOPT), Second Order perturbation Technique (SOPT) and Monte Carlo simulation.

Keywords: micromechanics model; random material properties; stochastic finite element method; Monte Carlo simulation

1. Introduction

An advanced SWCNT reinforced composite material offer great ability and excellent performance in widely used in aerospace and marine engineering. These material is compose with more than two phase of materials, SWCNR reinforced scheme is achieving high strength and stiffness to weight ratio and with good energy and sound absorption. The structural plates made of the composite material are increasingly used in many industrial applications such as aerospace, automotive and shipbuilding industries. In the literature review are carried out some researchers focused mead on bending, vibration and buckling characteristic of composite structure by using deterministic approach as follows. Jun *et al*. (2005) presented stochastic bending-torsion coupled response of axially loaded slender composite-thin-walled beams with closed cross-sections. Bounouara *et al*. (2016) studied a nonlocal zero-order shear deformation theory for free vibration of functionally graded Nano-scale plates resting on elastic foundation. Rahmzadeh *et al*. (2016) investigated effect of stiffeners on steel plate shear wall systems. The stochastic finite element approach is used for structural analysis. The few of researchers is developed stochastic model for buckling charachristic, Singh *et al*. (2001), Singh *et al*. (2009), Singh and Lal (2010), Lal *et al*. (2008). Lal *et al*. (2011) developed perturbation technique for effect of random system properties on bending response of thermo-mechanically loaded laminated composite plates. The stochastic post buckling analysis of laminated composite cylindrical shell panel subjected to hydro-thermo-mechanical loading were presented by Lal *et al*. (2011). They implemented the elastic and hydrothermal properties of the composite material considered to be dependent on temperature and moisture concentration using micromechanical approach. Kundu *et al*. (2014) presented a hybrid spectral and meta-modelling approach for the stochastic finite element analysis of structural dynamic systems. Chang (2014**)** developed a novel approach for uncertainty propagation and response statistics, estimation of randomly parameterized structural dynamic systems. They also studied stochastic dynamic finite element analysis of bridge-vehicle systems subjected to random material properties and loadings. Onkar *et al*. (2007) used probabilistic failure of laminated composite plates using the stochastic finite element method. Lal *et al*. (2012) developed a model for stochastic nonlinear failure analysis of laminated composite plates under compressive transverse loading. They also examined second ordered statistics of first-ply failure response of laminated composite plate with random material properties under random loading. the stochastic model is developed for composter structure, Shegokar and Lal (2013) stochastic nonlinear bending response, Singh *et al*. (2009) nonlinear free vibration, Singh *et al*. (2001) natural frequency, Singh *et al*. (2001) stability analysis, Lal *et al*. (2007) vibration, Lal and Singh *et al*. (2009) nonlinear vibration, Lal and Singh (2010) free vibration in thermal filed, Singh *et al* (2008), Pandit *et al*. (2009) bending analysis and Singh *et al*. (2009) vibration analysis of smart materials. The stochastic perturbation-based finite element for buckling

*Corresponding author, Ph.D.
E-mail: shivajigchavan@rediffmail.com
[a]Assistant Professor

ISSN: 1229-9367 (Print), 1598-6233 (Online)

statistics of FGM plates with uncertain material properties in thermal environments were investigated by Talha *et al*. (2014). Sasikumar *et al*. (2015) proposed stochastic model order reduction in uncertainty quantification of composite structures. Talha *et al*. (2015) presented for stochastic vibration characteristics of finite element modelled functionally gradient plates. The stochastic free vibration analyses of laminated composite plates using polynomial correlated function expansion were investigated by Chakraborty *et al*. (2016). Dey *et al*. (2016) studied the uncertain natural frequency analysis of composite plates by using polynomial neural network approach. The Spectral stochastic finite element vibration analyses of fibre-reinforced composites with random fibre orientation were proposed by Sepahvand (2016). Singh *et al*. (2010) proposed stochastic analysis of laminated composite plates resting on elastic foundation in the cases of post-buckling behaviour and nonlinear free vibration. Zhao *et al*. (2000) presented Neumann dynamic stochastic finite element method of vibration for structures with stochastic parameters to random excitation.

It is accomplished from the above mentioned literatures that the stochastic finite element implementation of SWCNTRC plate structure. The contribution of this paper is to provide a probabilistic tool for integrating structural material uncertainties in the analysis of the structures subjected to uniform transverse loadings. In the present work, efforts are made to develop a stochastic finite element model based on HSDT. The basic formulation in the present study is based on HSDT. A C^0 linear finite element method based on direct iterative procedure combined with the mean cantered FOPT, SOPT and MCS i.e., Stochastic finite element method (SFEM) with reasonable accuracy is employed to handle the randomness in material properties of SWCNTRC plate. The proposed probabilistic approach would be valid for material properties with small random dispersion as compared to mean values. This condition is satisfied with most of the engineering materials, fortunately, SWCNTs fall in this category. The main objective of the present research is aimed to evaluate second order statistics bending response of SWCNTRC plate. The paper is organized as follows Section 1 gives the brief introduction of related problem with suitable justification and patient literature survey based on deterministic and probabilistic analysis. The brief description of geometry configuration, material properties and the mathematical formulation of the problem using finite element method are given in Sections 2. In solution methodology of deterministic and stochastic finite element (perturbation technique) approach is presented in Section 3. Section 4 explains the result and discussion followed by validation studied with respect to various parameters with numerical examples and Section 5 complete the conclusion based on observation.

2. Theoretical formulation

In the present work, finite element formulation for SWCNTRC plate is based on HSDT because it represents the kinematics better, not require shear correction factors by Lal *et al*. (2012).

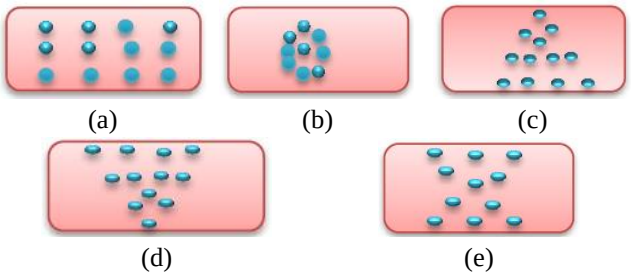

Fig. 1 The geometry and Configurations of FG-SWCNTRC plate for different grading (a) UD (b) FG-O (c) FG-A (d) FG-V (e) FG-X

2.1 Micromechanics analysis

In this section the Mori-Tanaka's method to the computation of the effective properties of SWCNTR composites. The mathematical mode taken from (Chavan and Lal 2017)

$$
\begin{aligned}
l &= \frac{E_m\left\{V_m v_m[E_m+2k_{CNT}(1+v_m)]+2V_{CNT}l_{CNT}(1-v_m^2)\right\}}{(1+v_m)[E_m(1+V_{CNT}-2v_m)+2V_m k_{CNT}(1-v_m-2v_m^2)]}\\
k &= \frac{E_m\left\{E_m V_m+2k_{CNT}(1+v_m)[1+V_{CNT}(1-2v_m)]\right\}}{2(1+v_m)[E_m(1+V_{CNT}-2v_m)+2V_m k_{CNT}(1-v_m-2v_m^2)]}\\
n &= \frac{E_m^2V_m(1+V_{CNT}-V_m v_m)+2V_m v_{CNT}(k_{CNT}n_{CNT}-l_{CNT}^2)(1-2v_m)}{(1+v_m)[E_m(1+V_{CNT}-2v_m)+2V_m k_{CNT}(1-v_m-2v_m^2)]}\\
&+\frac{E_m[2V_m^2k_{CNT}(1-v_m)+V_{CNT}n_{CNT}(1-2v_m+V_{CNT})-42V_m l_{CNT}v_m]}{2V_m k_{CNT}(1-v_m+v_m^2)+E_m(1-V_{CNT}+2v_m)}\\
p &= \frac{E_m[E_m V_m+2(1+V_{CNT})p_{CNT}(1+v_m)]}{2(1+v_m)[E_m(1+V_{CNT})+2V_m p_{CNT}(1+v_m)]}\\
m &= \frac{E_m[E_m V_m+2m_{CNT}(1+v_m)(3+V_{CNT}-4v_m)}{2(1+v_m)\{E_m[(V_m+4V_{CNT}(1-v_m)]+2V_m m_{CNT}(3-v_m-4v_m^2)]\}}
\end{aligned}
\tag{1}
$$

The Nano-composite properties can be calculated by using equation

$$
E_{11}=n-\frac{l^2}{k};\ E_{22}=\frac{4m(kn-l^2)}{kn-l^2+mn};\ G_{12}=2p;v_{12}=\frac{l}{2k}\cdot \tag{2}
$$

As shown in Fig. 1. Five types of FG-SWCNT reinforced composite plates with length (a) and width (b) and thickness (h) are considered. The SWCNTs are assumed to be uniaxial aligned, UD represents uniformed distributed and FG-O, FG-V, FG-X and FG-A are functionally graded distributions of SWCNTs. According to the distribution of uniaxial aligned SWCNTs, SWCNT constant by volume fraction V_{CNT} is expressed as (Chavan and Lal 2017)

$$V_{CNT}=V^* \quad \text{----------UD}$$

$$V_{CNT}=2\left(1-\frac{2|z|}{h}\right)V^* \quad \text{-------FG-O}$$

$$V_{CNT}=\left(\frac{2|z|+h}{h}+\right)V^* \quad \text{------FG-V}$$

$$V_{CNT}=4\left(\frac{|z|}{h}+\right)V^* \quad \text{----------FG-X}$$

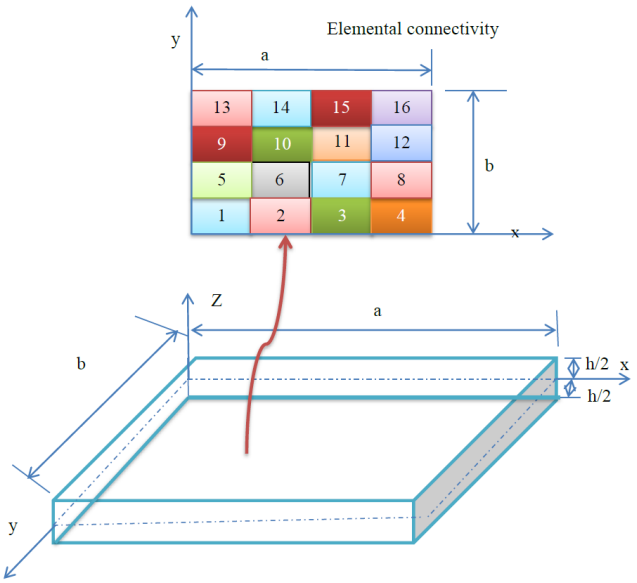

Fig. 2 SWCNT-Matrix reinforced composite plate

$$V_{CNT}=4\left(1-\frac{2|z|}{h}\right)V^{*}\text{--------FG-A}$$

$$V^{*}=\frac{W_{CNT}}{W_{CNT}+\left(\frac{\rho_{CNT}}{\rho_{m}}\right)(1-W_{CNT})} \tag{3}$$

2.2 Geometrical considerations of SWCNT composite plate

The single walled carbon nanotube composite plate subject to uniform transverse loadings with length (b), width (a), thickness (h) located in the three dimensional Cartesian coordinate system (*x*,*y*,*z*) as shown in Fig. 2. Where *x* and *y* are in the axial and tangential coordinate directions of the plate and *Z* is normal to the mid surface of the plate, respectively. It is assumed that perfect bonding exists between the SWCNTs and the matrix so that no slippage can occur at the interface and the strains experienced by the SWCNT, matrix and composite are equal. It is also assumed that the composite behaves like homogeneous material and the effect of the constituent materials (i.e., matrix and SWCNT) are noticed simultaneously.

2.3 Basic HSDT formulation

In the present study, higher order shear deformation theory (HSDT) using C^1 continuity is transformed into C^0 continuity by assuming derivatives of out-of-plane displacement as separate degree of freedom (DOFs). The displacement filed is take from Lal *et al.* (2011), can be written by

$$\begin{aligned}U_0&=u_0(x,y)+\left(z-\frac{4}{3h^2}z^3\right)\phi_x(x,y)-\frac{4}{3h^2}z^3\theta_x(x,y)\\V_0&=v_0(x,y)+\left(z-\frac{4}{3h^2}z^3\right)\phi_y(x,y)-\frac{4}{3h^2}z^3\theta_y(x,y)\\W_0&=w_0(x,y)\end{aligned} \tag{4}$$

Where U_0, V_0 and W_0 are displacements of any point in *x*, *y*, *z* coordinate axis and u_0, v_0, w_0 are the displacements of a corresponding point in the mid plane, ϕ_x and ϕ_y are the rotations at *z*=0 of normal about *y* and *x*, axes, respectively. θ_x and θ_y are the slopes along *x*, *y* axes respectively. The displacement field vector can be defined by

$$q(0)=\begin{pmatrix}u_0 & v_0 & w_0 & \theta_y & \theta_x & \phi_y & \phi_x\end{pmatrix} \tag{5}$$

For the SWCNTR composite plate of the present, bending analysis problem, the strain vector can be written as (Gadade *et al*. 2016, Chavan and Lal 2017),

$$\begin{Bmatrix}\varepsilon_x\\ \varepsilon_y\\ \varepsilon_z\\ \gamma_{xy}\\ \gamma_{xz}\\ \gamma_{yz}\end{Bmatrix}=\begin{Bmatrix}\varepsilon_1^0+z\left(k_1^0+z^2k_1^2\right)\\ \varepsilon_2^0+z\left(k_2^0+z^2k_2^2\right)\\ 0\\ \varepsilon_4^0+z^2k_4^2\\ \varepsilon_5^0+z^2k_5^2\\ \varepsilon_6^0+z\left(k_6^0+z^2k_6^2\right)\end{Bmatrix} \tag{6}$$

Here, the mid-plane strain vector can be defined as

$$\{\bar{\varepsilon}\}=\begin{Bmatrix}\varepsilon_1^0 & \varepsilon_2^0 & \varepsilon_6^0 & k_1^0 & k_2^0 & k_6^0 & k_1^2 & k_2^2 & k_6^2 & \varepsilon_4^0 & \varepsilon_5^0 & k_4^2 & k_5^2\end{Bmatrix}^T \tag{7}$$

Where, $\varepsilon_1^o=\frac{\partial u}{\partial x},\mathrm{k}_1^o=\frac{\partial \psi_x}{\partial x},\mathrm{k}_1^2=-\frac{4}{3h^2}\left(\frac{\partial^2 w}{\partial x^2}+\frac{\partial \psi_x}{\partial x}\right)$

$$\varepsilon_2^o=\frac{\partial u}{\partial y},\mathrm{k}_2^o=\frac{\partial \psi_y}{\partial y},\mathrm{k}_2^2=-\frac{4}{3h^2}\left(\frac{\partial^2 w}{\partial y^2}+\frac{\partial \psi_y}{\partial y}\right)$$

$$\varepsilon_4^o=\psi_y+\frac{\partial w}{\partial y},\mathrm{k}_4^2=-\frac{4}{h^2}\left(\psi_y+\frac{\partial w}{\partial y}\right)$$

$$\varepsilon_5^o=\psi_x+\frac{\partial w}{\partial x},\mathrm{k}_5^2=-\frac{4}{h^2}\left(\psi_x+\frac{\partial w}{\partial x}\right)$$

$$\varepsilon_6^o=\frac{\partial u}{\partial x}+\frac{\partial v}{\partial y},\mathrm{k}_6^o=\frac{\partial \psi_x}{\partial y}+\frac{\partial \psi_y}{\partial x},\mathrm{k}_6^2=-\frac{4}{3h^2}\left(\frac{\partial \psi_x}{\partial y}+\frac{\partial \psi_y}{\partial x}+2\frac{\partial^2 w}{\partial xy}\right)$$

The stress vector by considering σ_3=0 can be written as

$$\{\sigma\}=\begin{bmatrix}\sigma_1 & \sigma_2 & \tau_{21} & \tau_{23} & \tau_{31}\end{bmatrix}=\left[\bar{Q}\right]\{\varepsilon\} \tag{8}$$

The elemental potential energy of SWCNTRC plate is written as

$$U^{(e)}=\frac{1}{2}\int_V\{\varepsilon\}^{T(e)}\{\sigma\}^{(e)}dV=\frac{1}{2}\int_A\left(\{\varepsilon\}^{T(e)}\left[\bar{Q}\right]\{\varepsilon\}^{(e)}\right)dA=\frac{1}{2}\int_A\left(\{\bar{\varepsilon}\}^{T(e)}[D]\{\varepsilon\}^{(e)}\right)dA \tag{9}$$

The external work done of SWCNTRC plate can be written as

$$W=\int fq^T dv \tag{10}$$

Where, {*f*} is global load vector due to external mechanical loading.

2.4 Finite element model

The finite element model for the present SWCNTRC plate with the nine noded isoperimetric elements and seven degrees of freedom per node can be written as

$$q=\sum_{i=1}^{NN}N_iq_i;\quad x=\sum_{i=1}^{NN}N_ix_i;\ y=\sum_{i=1}^{NN}N_iy_i \tag{11}$$

Where, N_i is interpolation functions, q_i is a vector of unknown displacements of the i^{th} node, *NN* nodes per

element and x_i and y_i are the coordinates of the i^{th} node. The mid plane strain vector as given in Eq. (7) are used to express mid-plane displacement field with the help of strain-displacement relations (*B*-Matrix). The strain energy first computed for each element and summed over all the elements for computing the total strain energy.

The total potential energy of the SWCNTRC plate can be written as

$$\Pi = \sum_{e=1}^{E} U^{(e)} - W \tag{12}$$

The governing equation for the present case can be derived using the variation principle, which is a generalization of the principle of virtual displacement. For the deterministic analysis, the first variation of the total potential energy (Π) with respect to displacement must be zero.

$$\frac{\partial}{\partial \{q\}}(\Pi) = 0 \tag{13}$$

Substituting, Eq. (12) into Eq. (13), ones obtained

$$\left[K^d\right]\left\{q^d\right\} = \left\{F^d\right\} \tag{14}$$

The deterministic nodal displacement of SWCNTRC plate $\{q\}$ can be computed from Eq. (14)

3. Solution approach: Perturbation techniques

Being dependant on the random field variable such as material properties, plate thickness, volume fraction of SWCNT, the governing Eq. (14) of the present problem is random in nature. Therefore, there is a need to change the form of this equation and solve it by using a perturbation technique.

3.4 Zero, First and Second order perturbation technique (ZOPT, FOPT and SOPT)

The complete analysis of stochastic (Perturbation Technique) bending procedure of SWCNTRC plate is shown by a flow chart given in Fig. 3. The FOPT and SOPT are based on Taylor's series expansion to formulate the linear relationship between some characteristics of the random response and random structural parameters on the basis of perturbation approach. The applicability of this approach is limited to the problem where the coefficients of variations (COV) of input random variables are small. The most general form of governing in random environment is expressed by Gadade *et al*. (2016). The operational random system variables in the present case can be expanded using Taylor series about the mean values of random variables as up to second order. The random governing equation can be written as

$$\left[K^R\right]\left\{q^R\right\} = \left\{F^R\right\} \tag{15}$$

Where, $[K^R]$, $\{q^R\}$ and $\{F^R\}$ are represented as the random stiffness matrix, random displacement vectors and random force vectors respectively, *R* is known as random. The random variable is defined as: random variable $(RV)^R$= mean $(RV)^d$ - mean random variable (*RV*),

Operating random variables in the present problem are defined as (Shegokar and Lal 2013)

$$b^R = b^d + b^r;\ K = K^d + K^R;\ q = q^d + q^R;\ F = F^d + F^R, \tag{16}$$

The superscript '*d*' and '*r*' denote the mean and zero mean random part. The perturbation equations are taken from Gadade *et al*. (2016). The perturbation equation can be written as:

Zero order perturbation equation (ZOPT)

$$\left[K^d\right]\left\{q^d\right\} = \left\{F^d\right\} \tag{17}$$

First order perturbation equation (FOPT)

$$\left[\sum_{i=1}^{N}\left[\frac{\partial K^R}{\partial b_i^R}\right]b_i^R\right]\left\{\sum_{i=1}^{N}\left\{\frac{\partial q^R}{\partial b_i^R}\right\}b_i^R\right\} = \left\{\sum_{i=1}^{N}\left\{\frac{\partial F^R}{\partial b_i^R}\right\}b_i^R\right\} \tag{18}$$

Second order perturbation equation (ZOPT)

$$\left[\frac{1}{2}\sum_{i=1}^{N}\sum_{j=1}^{N}\left[\frac{\partial^2 K^R}{\left(\partial b_{ij}^R\right)^2}\right]\left(b_{ij}^R\right)^2\right]\left\{\frac{1}{2}\sum_{i=1}^{N}\sum_{j=1}^{N}\left[\frac{\partial^2 q^R}{\left(\partial b_{ij}^R\right)^2}\right]\left(b_{ij}^R\right)^2\right\} = \left\{\frac{1}{2}\sum_{i=1}^{N}\sum_{j=1}^{N}\left[\frac{\partial^2 F^R}{\left(\partial b_{ij}^R\right)^2}\right]\left(b_{ij}^R\right)^2\right\} \tag{19}$$

zeroth order Eq. (17) is the deterministic equation which can be solved by using convectional solution procedure and gives the mean displacements of the SWCNTRC plate. The First order perturbation equation (FOPT) Eq. (18) and Second order perturbation equation (ZOPT) Eq.(19) and solution of this equation provide the statistics of the bending response, which can be solved by using probabilistic approach like perturbation technique and Monte Carlo method. Using Taylor's series expansion, first order and second order stiffness matrix, displacement vector and force vectors respectively, can be expressed as (Gadade *et al*. 2015):

First order random stiffness matrix, force vector and displacement vector respectively

$$\left[K^R\right]^I = \sum_{i=1}^{N}\left[\frac{\partial K^d}{\partial b_i^R}\right]b_i^R,\ \left\{q^R\right\}^I = \sum_{i=1}^{N}\left\{\frac{\partial q^d}{\partial b_i^R}\right\}b_i^r,\ \left\{F^R\right\}^I = \left\{\sum_{i=1}^{N}\left\{\frac{\partial F^d}{\partial b_i^R}\right\}b_i^R\right\} \tag{20}$$

Second order random stiffness matrix, force vector and displacement vector respectively

$$\left\{F^R\right\}^{II} = \left\{\frac{1}{2}\sum_{i=1}^{N}\sum_{j=1}^{N}\left[\frac{\partial^2 F^d}{\left(\partial b_{ij}^R\right)^2}\right]\left(b_{ij}^R\right)^2\right\}$$

$$\left\{q^R\right\}^{II} = \left\{\frac{1}{2}\sum_{i=1}^{N}\sum_{j=1}^{N}\left[\frac{\partial^2 q^d}{\left(\partial b_{ij}^R\right)^2}\right]\left(b_{ij}^R\right)^2\right\}\ \left[K^R\right]^{II} = \frac{1}{2}\sum_{i=1}^{N}\sum_{j=1}^{N}\left[\frac{\partial^2 K^d}{\left(\partial b_{ij}^R\right)^2}\right]\left(b_{ij}^R\right)^2 \tag{21}$$

The first order elemental random stiffness matrix $[k^R]^I$ is defined by

$$\left[k^R\right]^I = \left\{B_q\right\}\left[D^R\right]^I\left\{B_q\right\}^T \tag{22}$$

Where,

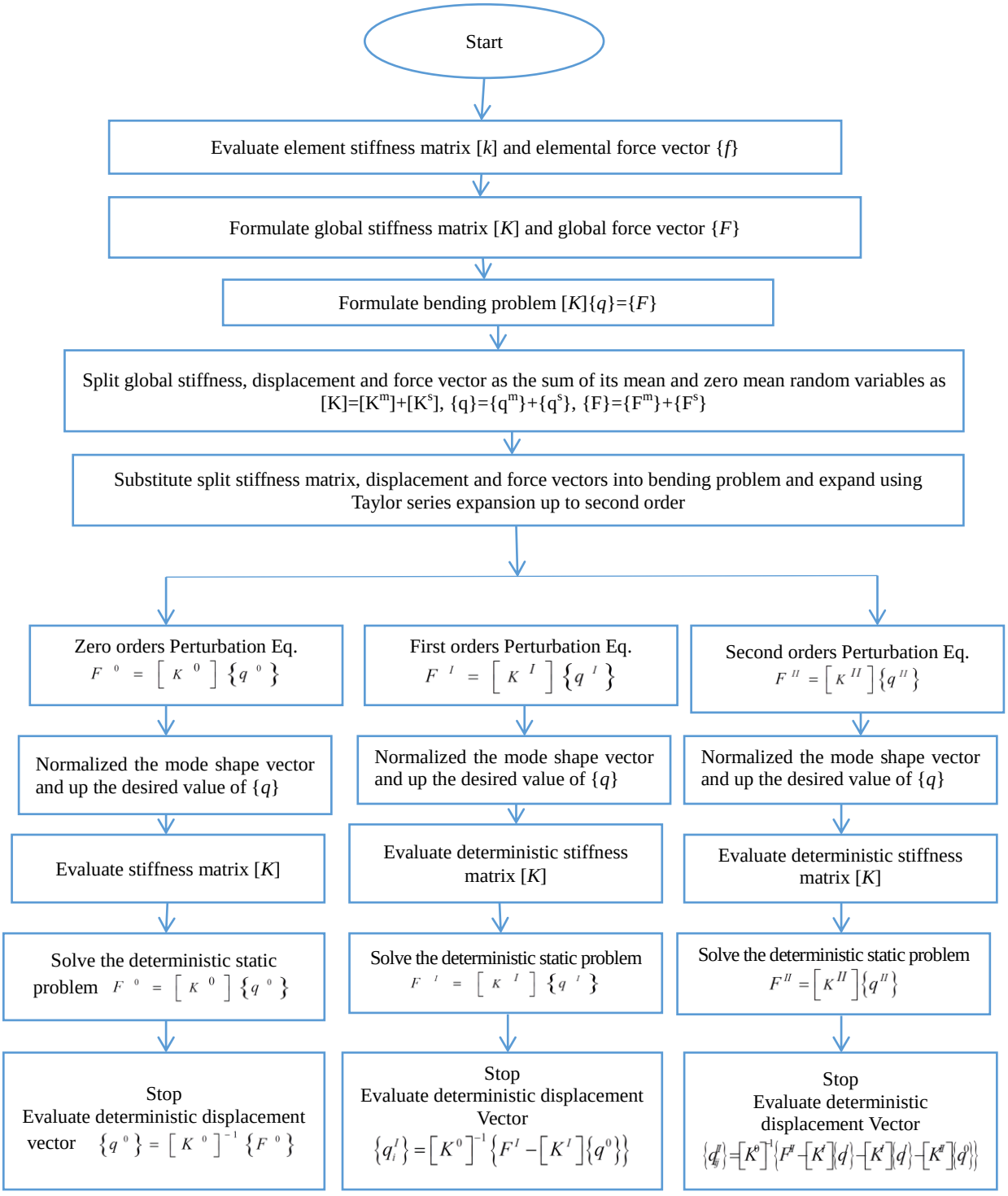

Fig. 3 Schematic flow chart of stochastic (Perturbation Technique) bending analysis

$$\{B_4\}=\begin{bmatrix}
\partial/\partial x & 0 & 0 & 0 & 0 & 0 & 0\\
0 & \partial/\partial y & 0 & 0 & 0 & 0 & 0\\
\partial/\partial y & \partial/\partial x & 0 & 0 & 0 & 0 & 0\\
0 & 0 & 0 & 0 & 0 & 0 & C1\partial/\partial x\\
0 & 0 & 0 & 0 & 0 & C1\partial/\partial y & 0\\
0 & 0 & 0 & 0 & 0 & C1\partial/\partial x & C1\partial/\partial y\\
0 & 0 & 0 & 0 & -C4\partial/\partial x & 0 & -C2\partial/\partial x\\
0 & 0 & 0 & -C4\partial/\partial y & 0 & -C2\partial/\partial y & 0\\
0 & 0 & 0 & -C4\partial/\partial x & -C4\partial/\partial y & -C2\partial/\partial x & -C2\partial/\partial y\\
0 & 0 & C1\partial/\partial y & 0 & 0 & C1 & 0\\
0 & 0 & C1\partial/\partial x & 0 & 0 & 0 & C1\\
0 & 0 & 0 & -3C4 & 0 & -3C2 & 0\\
0 & 0 & 0 & 0 & -3C4 & 0 & -3C2
\end{bmatrix};$$

and

$$\left[D^R\right]^I=\begin{bmatrix}
\left[A_1^R\right] & \left[A_2^R\right] & \left[A_3^R\right] & \left[A_4^R\right]\\
\left[B_1^R\right] & \left[B_2^R\right] & \left[B_3^R\right] & \left[B_4^R\right]\\
\left[C_1^R\right] & \left[C_2^R\right] & \left[C_3^R\right] & \left[C_4^R\right]\\
\left[E_1^R\right] & \left[E_2^R\right] & \left[E_3^R\right] & \left[E_4^R\right]
\end{bmatrix}$$

The $[k^R]^I$ is detail expanded in Appendix.

The elemental random force vector $\{F^R\}^I$ is defined by

$$\left\{F^R\right\}^I=\left[H_f\right]\left[P^R\right]^I \tag{23}$$

Where,

$$\left[H_f\right]=\begin{bmatrix} shape(i) & 0 & 0 & 0 & 0 & 0 & 0 \\ 0 & shape(i) & 0 & 0 & 0 & 0 & 0 \\ 0 & 0 & shape(i) & 0 & 0 & 0 & 0 \\ 0 & 0 & 0 & shape(i) & 0 & 0 & 0 \\ 0 & 0 & 0 & 0 & shape(i) & 0 & 0 \\ 0 & 0 & 0 & 0 & 0 & shape(i) & 0 \\ 0 & 0 & 0 & 0 & 0 & 0 & shape(i) \end{bmatrix}$$

For i=1, 2, 3…., 9

$$\left[P^R\right]^I=\begin{bmatrix} 0 & 0 & \dfrac{Q_0}{b_i^R} & 0 & 0 & 0 & 0 \end{bmatrix}$$

Similarly, the second order elemental random stiffness matrix $[k^R]^{II}$ and random force vectors are defined by

$$\left[k^R\right]^{II}=\left\{B_q\right\}\left[D^R\right]^{II}\left\{B_q\right\}^T \text{ and } \left\{F^R\right\}^{II}=\left[H_f\right]\left[P^R\right]^{II} \quad (24a)$$

$[D^R]^{II}$ matrix is detail expanded in Appendix-1 and random force vector is expressed by

$$\left[P^R\right]^{II}=\begin{bmatrix} 0 & 0 & \dfrac{Q_0}{2\left(b_i^R\right)^2} & 0 & 0 & 0 & 0 \end{bmatrix} \quad (24b)$$

$$\left[D^R\right]^{II}=\begin{bmatrix} \left[A_{11}^R\right] & \left[A_{12}^R\right] & \left[A_{13}^R\right] & \left[A_{14}^R\right] \\ \left[B_{21}^R\right] & \left[B_{22}^R\right] & \left[B_{23}^R\right] & \left[B_{24}^R\right] \\ \left[C_{31}^R\right] & \left[C_{32}^R\right] & \left[C_{33}^R\right] & \left[C_{34}^R\right] \\ \left[E_{41}^R\right] & \left[E_{42}^R\right] & \left[E_{43}^R\right] & \left[E_{44}^R\right] \end{bmatrix} \quad (24c)$$

The Eqs. (22)-(24) determines the elemental random stiffness matrix and force vectors for first order and second order perturbation equation respectively. After that all elemental random matrix are assemble and obtained total system of random stiffness matrix and random force vector respectively. The random displacement field of SWCNTRC plate for ZOPT, FOPT and SOPT equations respectively is taken from Gadade *et al*. (2016), it can be defined by

$$\left\{q^R\right\}^0=\left[K^d\right]^{-1}\left\{F^d\right\} \quad (25)$$

$$\left\{q^R\right\}^{II}=\left[K^d\right]^{-1}\left\{\left[F^R\right]^I-\left[\left[K^R\right]^I\right]\left\{q^d\right\}\right\} \quad (26)$$

$$\left\{q^R\right\}^{II}=\left[K^d\right]^{-1}\left\{\left[F^R\right]^{II}-\left[K^R\right]^R\left\{q^R\right\}^I-\left[K^R\right]^{II}-\left[K^R\right]^{II}\left\{q^d\right\}^I\right\} \quad (27)$$

Eq. (25) is denoted as zero order displacement of SWCNTRC plate. $\{\}^0$; $\{\}^I$; $\{\}^{II}$ zero order, first order and second order of SWCNTRC deflection vector respectively. The Eq. (26) and Eq. (27) is being first order and second order represents its random equivalent and solution of these equations give the statistics of the mean linear static deflection of SWCNTRC plate acted upon by uniform transverse loading. Total deflection response of SWCNTRC for ZOPT, FOPT and SOPT respectively is given by (Lal *et al*. 2011)

$$\left\{q_{total}\right\}=\left\{q^d\right\}+\left\{q^R\right\}^{0,I,II} \quad (28)$$

In the present analysis, the uncorrelated random variable is taken into consideration. Therefore, covariance is equal to the variance. The standard deviation and correlation coefficient matrix is explained by Gadade *et al*. (2016)

$$\left[\sigma_b\right]=\begin{bmatrix} \sigma_{b1} & \dots & \dots & 0 \\ 0 & \sigma_{b2} & \dots & 0 \\ \dots & \dots & \dots & \dots \\ 0 & \dots & \dots & \sigma_{bm} \end{bmatrix} \text{ and } \left[\rho_{ij}\right]=\begin{bmatrix} 1 & \rho_{12} & \dots & \rho_{1m} \\ \rho_{21} & 1 & \dots & \rho_{2m} \\ \dots & \dots & \dots & \dots \\ \rho_{m1} & \rho_{m2} & \dots & 1 \end{bmatrix} \quad (29)$$

Where, Random variables b_i (i=1, 2…m), $[\sigma_b]$ is a standard deviation (SD) of random variables $[\rho_{ij}]$ is a matrix of the correlation coefficient matrix and m is the number of random variables. The variance of the deflection of SWCNTRC plate can be written as

$$COV\{q\}^0=\left(\frac{\left\{q^R\right\}^0}{b_i^R}\right)[\sigma_\alpha]\left[\rho_{ij}\right][\sigma_\alpha]\left(\frac{\left\{q^R\right\}^0}{b_i^R}\right)^T \text{ ZOPT}$$

$$COV\{q\}^I=\left(\frac{\partial\left\{q^R\right\}^I}{\partial b_i^R}\right)[\sigma_\alpha]\left[\rho_{ij}\right][\sigma_\alpha]\left(\frac{\partial\left\{q^R\right\}^I}{\partial b_i^R}\right)^T \text{ FOPT}$$

$$COV\{q\}^{II}=\left(\frac{\partial^2\left\{q^R\right\}^{II}}{\left(\partial b_i^R\right)^2}\right)[\sigma_\alpha]\left[\rho_{ij}\right][\sigma_\alpha]\left(\frac{\partial^2\left\{q^R\right\}^{II}}{\left(\partial b_i^R\right)^2}\right)^T \text{ SOPT} \quad (30)$$

In this formulation Eq. (30) is represented the covariance of central SWCNTRC plate of deflection in the form of standard deviation and random variables. It is evident from Eq. (30), the coefficients of variance of transverse central deflection obtained by using the zero order, first order and second order perturbation techniques with all random variables in material properties, loading, and volume fraction of SWCNTs.

3.5 Monte Carlo simulation (MCS)

In general MCS is used to check the statistic quantity and is very costly, since it needs marvellous repeated computation for all different samples. The Monte Carlo simulation (MCS) is relies on direct use of computer and simulates an experiment. The mean or expected value of a function $f(\boldsymbol{x})$ of a n-dimensional random variable vector $\boldsymbol{x}$, whose joint probability density function is given by ($\boldsymbol{x}$) expressed as

$$\mu_f=E\left[f(x)\right]=\int_\Omega f(x)\phi(x)dx \quad (31)$$

The above multidimensional integral is difficult to evaluate analytically for many types of joint density functions. Also, the integrand function $f(x)$ may not be available in analytical form and can only be calculated numerically. The above integral can be evaluated using MCS approach. In MCS approach, N sample points are generated using a suitable sampling approach in the n-dimensional random variable. The N samples drawn must follow the distribution specified by $\varphi(x)$. When we have the N samples for x, the function in the integrand $f(x_i)$ is evaluated at each of the N-sampling points, x_i. The integral for the expectable value, then takes the form of averaging operator shown below.

$$\overline{\mu}_f=E\left[f(x)\right]=\frac{1}{N}\sum_{i=1}^{N}f(x_i) \quad (32)$$

Similarly the variance of the random function $f(x)$ is

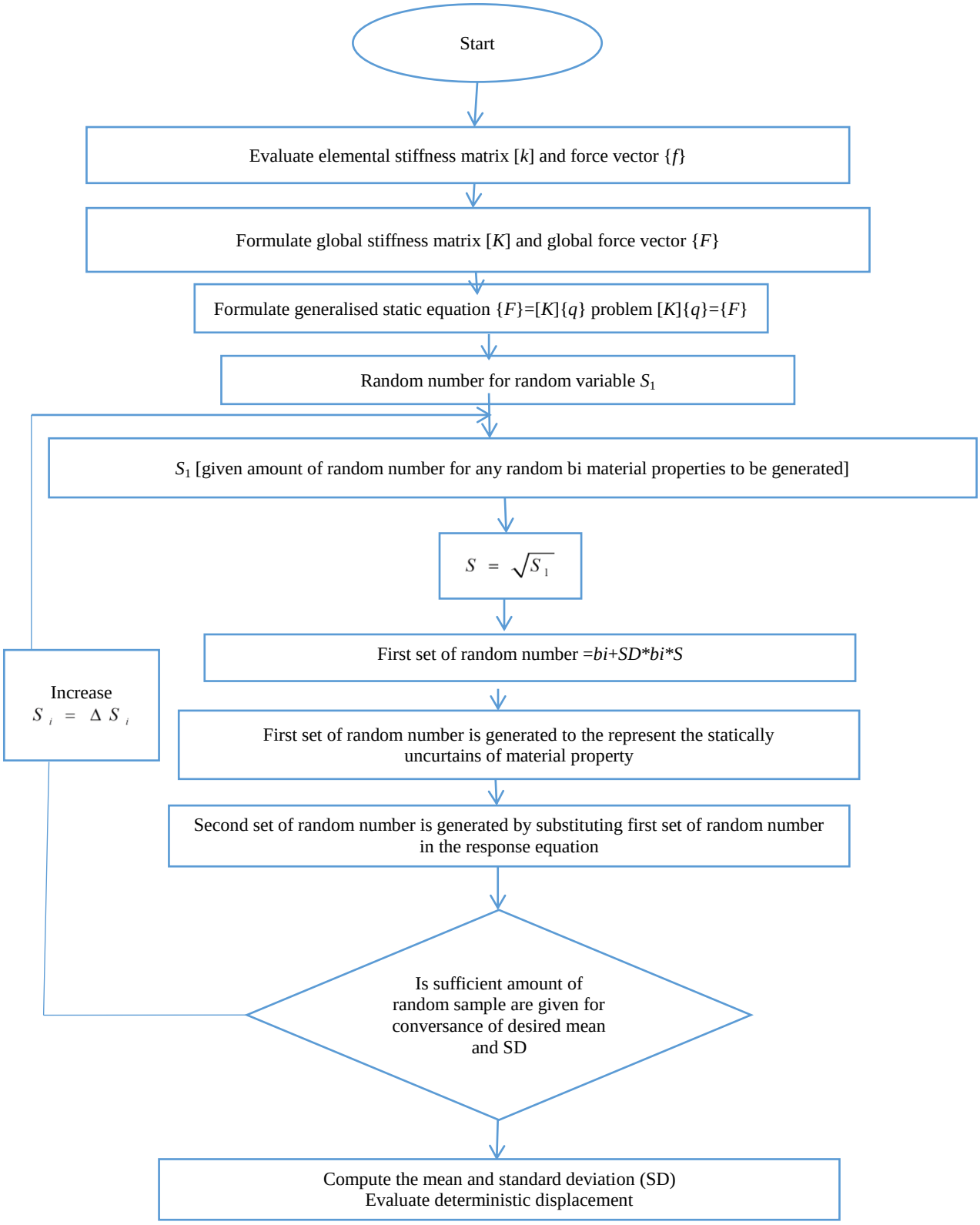

Fig. 4 Monte Carlo simulation (MCS) flow chart

given by the integral below

$$\sigma_f^2 = Var\left[f(x)\right] = \int_{\Omega} \left(f(x) - \mu_f\right)^2 \phi(x)\, dx \tag{33}$$

The above integral can be replaced by the following addition, when calculated using sampled values in MCS.

$$\hat{\sigma}_f^2 = Var\left[f(x)\right] = \frac{1}{N-1}\sum_{i=1}^{N}\left(f(x_i) - \mu_f\right)^2 \tag{34}$$

The task of the MCS approach lies in generating the random sample points that follow the distribution similar in form to the integrand. In the present study, the number of

samples taken as N=4000. Keeping in mind that the restriction of MCS, it is used only for validation purpose to handle random properties. The detailed analysis of MCS procedure is shown by flow chart given in Fig. 4. This flow chart to commute the standard deviation of SWCNTRC deflection it is defined as

$$S = \sqrt{S1} \tag{35}$$

Where S= standard deviation and $S1$= variance of central deflection of SWCNTRC plate. Stranded deviation is square root of covariance of central deflection of SWCNTRC. After that COV of deflection of SWCNRC plate using MCS can be defined by

$$COV,(q)_0 = \frac{S}{Mean} \tag{36}$$

4. Results and discussion

In the present study, a finite element code has been developed in MATLAB software on the basis of HSDT. The finite element code in MATLAB is explained in detail by Kwon *et al*. (2011) for bending analysis using nine noded isoperimetric element formulations. The SWCNTRC plate considered in the present bending analysis is discretised by (4X4) using a nine noded isoperimetric element, with 63 DOFs per element and elemental connectivity as shown in Fig. 2. Numerical results are presented in this section for SWCNTRC plate subjected to uniform transverse loading P=0.1 MPa. The SWCNTRC plates are made of carbon nanotube embedded into polymer matrix.

Mechanical properties of matrix are assumed to be E_m=3.0215 GPa and v_m=0.3.

SWCNTs are chosen as reinforcement and material properties of the SWCNT are as follows:

SWCNT armchair (5, 5): (Length=4.9405 nm, Diameter =0.718 nm, Thickness= 0.035 nm)

$$E_{11}^{CNT} = 58.64GPa, E_{22}^{CNT} = E_{33}^{CNT} = 5.11GPa,$$
$$\mathrm{G}_{12}^{CNT} = 1.605GPa v_{12}^{CNT} = v_{21}^{CNT} = 0.33, v_{23}^{CNT} = 0.48$$

SWCNT armchair (10, 10): (Length=9.26 nm, Diameter =1.36 nm, Thickness= 0.067 nm)

$$E_{11}^{CNT} = 103.23GPa, E_{22}^{CNT} = E_{33}^{CNT} = 6.05GPa,$$
$$\mathrm{G}_{12}^{CNT} = 2.11GPa, v_{12}^{CNT} = v_{21}^{CNT} = 0.33, v_{23}^{CNT} = 0.51$$

SWCNT armchair (15, 15): (Length=14.35 nm, Diameter =2.11 nm, Thickness= 0.104 nm).

$$E_{11}^{CNT} = 131.8GPa, E_{22}^{CNT} = E_{33}^{CNT} = 5.75GPa,$$
$$\mathrm{G}_{12}^{CNT} = 2.49GPa, v_{12}^{CNT} = v_{21}^{CNT} = 0.32, v_{23}^{CNT} = 0.36$$

SWCNT armchair (20, 20): (Length=19.13 nm, Diameter =2.81 nm, Thickness= 0.138 nm)

$$E_{11}^{CNT} = 158.24GPa, E_{22}^{CNT} = E_{33}^{CNT} = 4.17GPa,$$
$$\mathrm{G}_{12}^{CNT} = 2.11GPa, v_{12}^{CNT} = v_{21}^{CNT} = 0.32, v_{23}^{CNT} = 0.78$$

The geometric properties of SWCNTRC plate, is considered as, a=10 mm, b=10 mm and h=1.35 mm, uniform transverse loading P=0.1 MPa, side to thickness ratios (a/h)=20, 30, 50, 75 and 100 and Volume fraction SWCNT (V_{CNT})=0.11, 0.17 0.2 0.22 and 0.25. The effective material properties of SWCNTRC plate are estimated using Eq. (2). The mathematical model of UD and FG-O, FG-X, FG-V, FG-A plates are taken from (Chavan and Lal, 2017). The following dimensionless linear transverse mean central deflection has been used in this study: W_0=w/h.

In the present study, various combinations of boundary edge support conditions, namely, simply supported (SSSS), clamped and combination of clamped and simply supported have been used. The boundary condition can be written as:

a) All edges are simply supported edges (SSSS)

$u = v = w = \psi_y = \theta_y = 0$ at x=0 and a. ; $u = v = w = \psi_x = \theta_x = 0$ at y=0 and b.

b) All edges are clamped (CCCC)

$u = v = w = \psi_x = \psi_y = \theta_x = \theta_y = 0$ at x=0, a and y=0, b

c) Two opposite edges clamped and other two simply supported (CSCS):

$$u = v = w = \psi_x = \psi_y = \theta_x = \theta_y = 0, at\ x = 0\ and\ y = 0$$

$u = w = \psi_y = \theta_y = 0\ at\ x = a$ and $u = w = \psi_x = \theta_x = 0\ at\ y = b$

Once estimated the values of E_{11}, E_{22}, E_{33} and G_{12}, and G_{23} for UD and FG plate, then putting these values in stiffness matrix and applying boundary conditions to evaluate the deterministic deflection of SWCNTRC-FG plates. The changes in input material properties of COC are varying from 0 to 10%. The basic random input variables such as E_{11}, E_{22}, G_{12}, G_{13}, G_{23}, V_{12}, and P are ordered and defined as: $b_1 = E_{11},\ b_2 = E_{22},\ b_3 = G_{12},\ b_4 = G_{13},\ b_5 = G_{23}\ b_6 = v_{12}\ b_7 = P$

The random stiffness matrix is function of random variable system. The results obtained by proposed stochastic approach as described by Eq. (30) for ZOPT, FOPT SOPT. The Eq. (35) has been obtained standard deviation by using MCS technique and SD substitutes in Eq. (36) we get COV of deflection of SWCNTRC plate, which are listed in Table 1. Table 1 shows the effect of the variation of random properties of system $b_{i,}$ [{(i=1-7)}= 0.1] on the COV of deflection of the SWCNTRC plate subjected to uniform transvers loading (q0=0.1 MPa) for different a/h and volume fraction. The result shows that COV, W_0 of SWCNTRC plate is increases with increase in a/h ratio for ZOPT, FOPT, SOPT and MCS whereas it is COV, W_0 decreases with increase in volume fraction of SWCNT. The result also shows that COV, W_0 of ZOPT is lower as compared the FOPT, SOPT and MCS. Table 2 shows the effect of the variation of random properties of

Table 1 The COV of central deflection for ZOPT, FOPT, SOPT and MCS with varying a/h and V_{CNT}.

a/h	ZOPT	FOPT	SOPT	MCS	V_{CNT}	ZOPT	FOPT	SOPT	MCS
10	0.02951	0.0683	0.0691	0.0688	0.11	0.0413	0.0859	0.0875	0.0865
20	0.02956	0.0837	0.0848	0.08424	0.17	0.03065	0.0837	0.0848	0.08428
30	0.02963	0.0897	0.091	0.09033	0.2	0.0274	0.0827	0.0836	0.08313
40	0.02971	0.0921	0.0934	0.09276	0.25	0.02356	0.0811	0.0819	0.0817
50	0.02982	0.0933	0.0946	0.09397	0.3	0.02092	0.0798	0.0805	0.08012
60	0.02995	0.0939	0.0952	0.09453	0.45	0.01652	0.077	0.0775	0.07729
70	0.0301	0.0943	0.0956	0.09498	0.5	0.01568	0.0764	0.0769	0.07661
80	0.03029	0.0946	0.0959	0.09527					
90	0.03065	0.0948	0.0961	0.09542					
100	0.03499	0.095	0.0963	0.09568					

Table 2 variation of random system property for COV, b_i [(i=1-7) =0.10] on Mean and COV of central deflection of SWCNTRC plates

	UD		FG-O		FG-V		FG-X		FG-A	
a/h	Mean	COV	Mean	COV	Mean	COV	Mean	COV	Mean	COV
20	0.1602	0.0726	1.0134	0.4041	0.1561	0.0723	0.16	0.0727	0.956	0.4282
30	0.1358	0.0806	1.4977	0.1228	0.1319	0.0805	0.1356	0.0807	1.8195	0.1958
50	0.1188	0.0855	0.5019	0.1367	0.1151	0.0856	0.1186	0.0856	2.0898	0.1852
75	0.11	0.0886	0.5463	0.1243	0.1065	0.0883	0.1098	0.0884	2.1624	0.1826
100	0.1057	0.0937	0.559	0.1262	0.1022	0.0912	0.1054	0.0912	2.1867	0.18
V_{CNT}										
0.11	0.8865	0.155	20.1965	0.8805	0.166	0.1875	0.1619	0.1546	1.9935	0.3103
0.17	6.7798	0.135	17.9368	0.7832	0.1261	0.094	0.1234	0.0964	2.8177	0.2427
0.2	0.7829	0.1249	4.8778	0.2913	0.1153	0.092	0.1131	0.0947	3.4852	0.1861
0.22	0.2472	0.1004	3.2745	0.2233	0.11	0.043	0.1081	0.094	4.1965	0.1105
0.25	0.1298	0.0865	2.1867	0.180	0.1039	0.035	0.1024	0.0933	6.0502	0.0749
Index										
(5,5)	0.4813	0.8999	0.8267	0.2567	0.7281	0.1601	0.7149	0.2501	0.0587	0.3024
(10,10)	0.4715	0.5077	0.7117	0.1899	0.3041	0.1301	0.2977	0.1334	0.9668	0.2014
(15,15)	0.1198	0.1036	0.5268	0.1332	0.1261	0.097	0.1234	0.0964	0.8177	0.1227
(20,20)	0.0898	0.0132	0.3464	0.0285	0.0838	0.0085	0.0834	0.0083	0.1297	0.0998

	Armchair (5,5)		Armchair(10,10)		Armchair (15,15)		Armchair (20,20)	
a/h	Mean	COV	Mean	COV	Mean	COV	Mean	COV
20	1.1389	0.2048	0.5709	0.0851	7.2513	0.0760	0.0561	0.0478
30	1.0792	0.245	0.5265	0.0871	7.1196	0.0778	0.0574	0.0289
50	1.0403	0.271	0.4918	0.0904	6.9438	0.0803	0.0683	0.0183
75	1.0264	0.309	0.4772	0.0954	6.8236	0.0853	0.0793	0.0147
100	1.0213	0.473	0.4715	0.1077	6.7798	0.0999	0.0898	0.0132
V_{CNT}								
0.11	1.2062	0.7005	0.6075	0.1844	0.2765	0.1548	0.0924	0.0181
0.17	1.0213	0.6599	0.4715	0.5277	6.7798	0.4236	0.0898	0.0132
0.2	0.9522	0.498	0.4273	0.1997	0.7829	0.1819	0.0887	0.0118
0.22	0.9123	0.3398	0.4032	0.1113	0.2472	0.1004	0.0879	0.0111
0.25	0.86	0.0998	0.3731	0.114	0.1298	0.0565	0.0869	0.0102

system $b_{i,}$ [{(i=1-7)}=0.1] on the mean and COV of deflection of the SWCNTRC plate subjected to uniform transvers loading (q0=0.1 MPa) for different FG and volume fraction of SWCNT. Shows the effect of the variation of all random system as input parameter, $b_{i,}$ [{(i=1-7)}=0.1] on the mean and COV of deflection for the SWCNTRC plate by changing *a/h*, volume fraction and SWCNT chirality index SWCNTRC plate under lateral pressure loading. The results show the effect of variation of *a/h* on COV, W_0 for UD, FG-O, FG-V, and FG-X and FG-A. It can be seen that the COV, W_0 increase with increase in *a/h* ratio. The maximum COV, *W*0, are present in FG-A and FG-O, Therefor FG-A and FG-O plates are more sensitive. The range of COV, W_0 is 0.4282 to 0.0723 for UD, FG-O, FG-V, FG-X and FG-A by changing the *a/h*. The results shows that the effect of change in volume fraction of SWCNT on COV of central deflection for UD, FG-O, FG-V, FG-X and FG-A of Nano-composite plate. The COV, W0 of SWCNTRC plate is decrease with increase in Volume fraction of SWCNTs. The range of COV, W_0 is 0.888 to 0.035 for UD, FG-O, FG-V, FG-X and FG-A by changing the volume fraction of SWCNTs. The results show the effect of variation of chiral index (*m*, *n*) on COV, W_0 for UD, FG-O, FG-V, FG-X and FG-A plates. It can be seen that COV of SWCNTRC plate is decrease with increase in chiral index (*m*, *n*), whereas, the increase in dimension of SWCNT by changing the chiral index. The range of COV, W_0 is 0.899 to 0.0085 for UD, FG-O, FG-V, FG-X and FG-A by changing the chiral index. The results show the effect of variation of *a/h* on COV, W_0 for Armchair (5, 5), Armchair (10, 10), Armchair (15, 15) and Armchair (20, 20). The COV, W_0 of SWCNTRC plate is increase with increase in a/h ratio. The range of COV, W_0 is 0.473 to 0.0478 for Armchair (5, 5), Armchair (10, 10), Armchair (15, 15) and Armchair (20, 20) by changing the a/h ratio. The results show the effect of variation of volume fraction on COV, W_0 for Armchair (5, 5), Armchair (10, 10), Armchair (15, 15) and Armchair (20, 20). COV, W0 of SWCNTRC plate is decrease with increase in volume fraction of SWCNTs. The range of COV, W_0 is 0.7005 to 0.0102 for Armchair (5, 5), Armchair (10, 10), Armchair (15, 15) and Armchair (20, 20) by changing volume fraction of SWCNTs. Fig. 5 shows the comparison of present normal distribution of deflection of SWCNTRC plate subjected to uniform transvers loading (*P*) for FOPT, SOPT and MCS method. The results obtained by present perturbation technique (FOPT and SOPT) approach show fairly good agreement with the results of MCS for COV of deflection of SWCNTRC plate. However, COV of SOPT results is slightly more than the MCS and FOPT results, due to SOPT is a second order derivative of stiffness. Fig. 6 depicts the effect of random change in all random variables $b_{i,}$ [{(i=1-7)}=0.1] with different grading SWCNT on COV of deflection of SWCNTRC plate under lateral pressure with (V_{CNT}=0.17, *a*=*b*=1, *a/h*=20 to100). The result shows that the COV, W_0 of FG-A plate is maximum as compared to other types of UD and FG plates. Hence, the FG-A plate is more sensitive as compare to other types of plates. Fig. 7 shows the effect of random change in all random variables $b_{i,}$ [{(i=1-7)}=0.1] with different grading SWCNT on COV

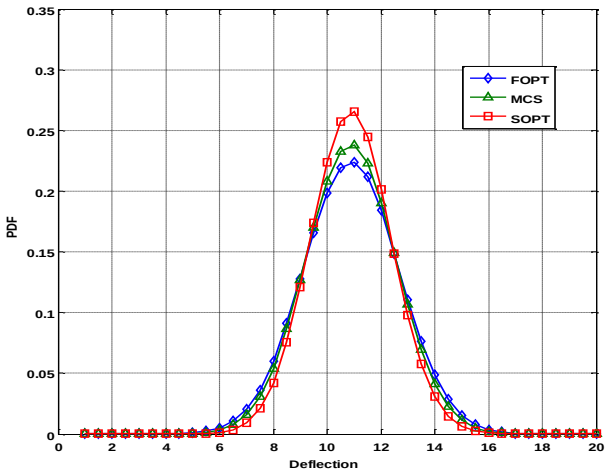

Fig. 5 Validation of present stochastic FEM approach (FOPT, SOPT) with MCS results of SWCNTR composite plate subjected lateral loading having clamped support condition

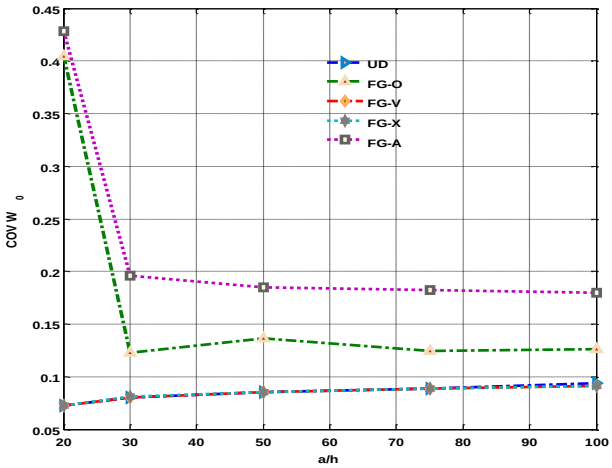

Fig. 6 Effect of random change in all input parameters taken at a time *with* COC=0.1 and different width-to-thickness ratio (*a/h*) of square SWCNTRC plates on CCCC support condition

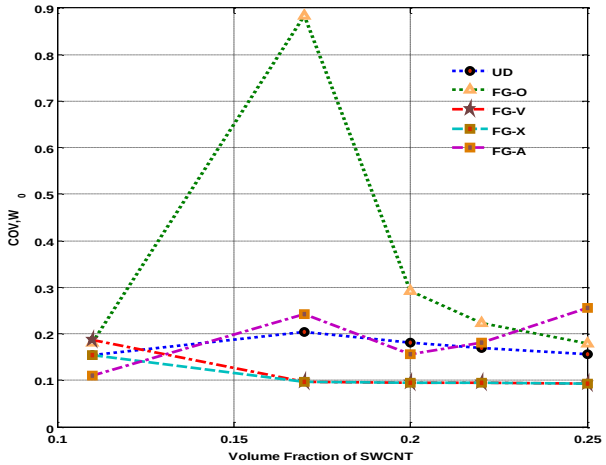

Fig. 7 Effect of random change in all input parameters taken at a time with COC=0.1 and different volume fraction of SWCNT of square SWCNTRC plates on CCCC support condition

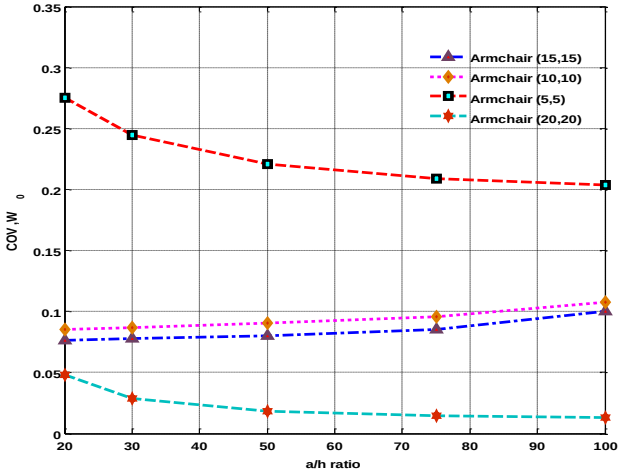

Fig. 8 Effect of random change in all input parameters taken at a time *with* COC=0.1 and different width-to-thickness ratio (*a/h*) of various SWCNT configuration plates on CCCC support condition

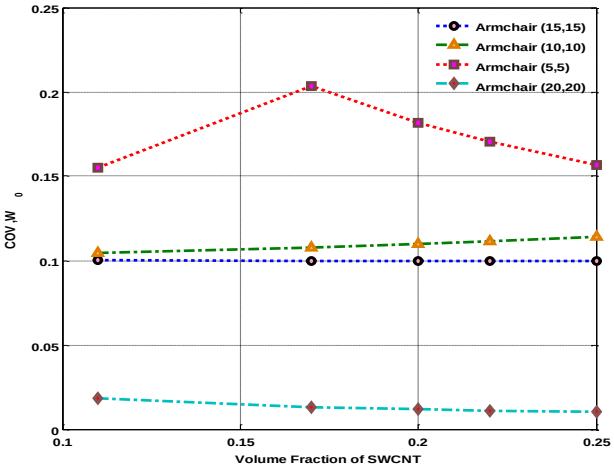

Fig. 9 Effect of random change in all input parameters taken at a time *with* COC=0.1 and different SWCNT volume fraction of various SWCNT configuration plates on CCCC support condition

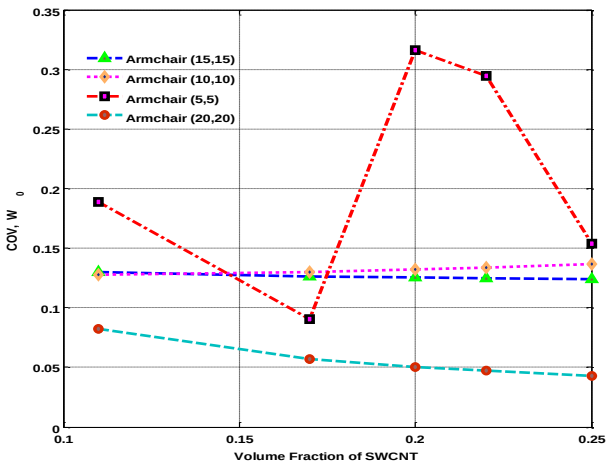

Fig. 10 Effect of random change in all input parameters taken at a time *with* COC=0.1 and different SWCNT volume fraction of various SWCNT configuration plates on SSSS support condition

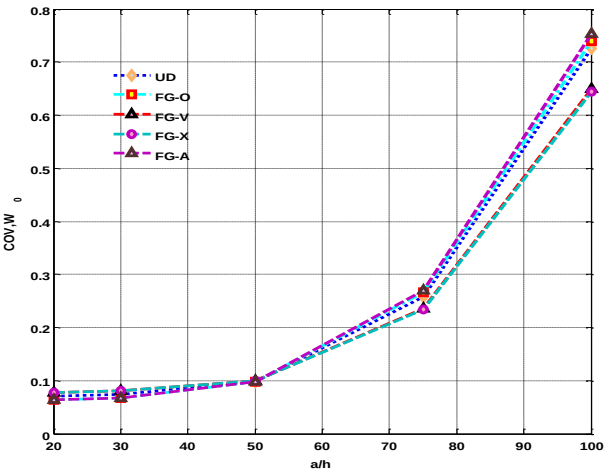

Fig. 11 Effect of random change in all input parameters taken at a time *with* COC=0.1 and different width-to-thickness ratio (*a/h*) of various SWCNT-FG plates on CFCF support condition

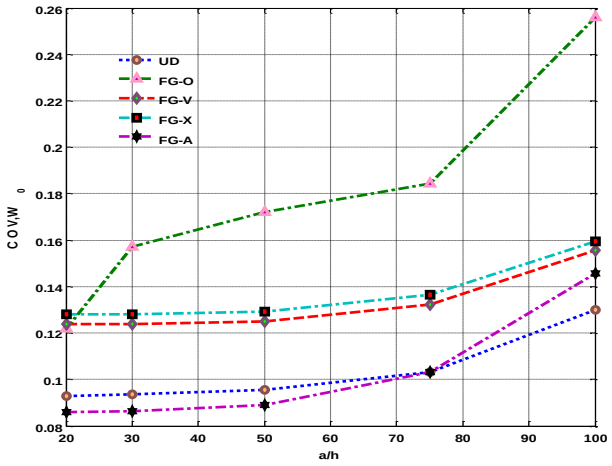

Fig. 12 Effect of random change in all input parameters taken at a time *with* COC=0.1 and different width-to-thickness ratio (*a*/*h*) of various SWCNT-FG plates on SSSS support condition

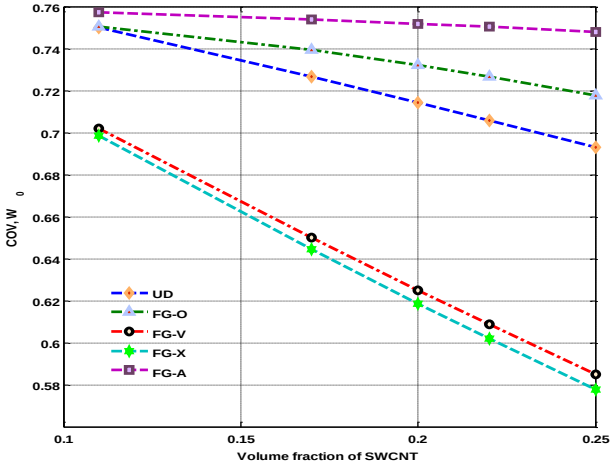

Fig. 13 Effect of random change in all input parameters taken at a time *with* COC=0.1 and different SWCNT volume fraction of various SWCNT-FG plates on CFCF support condition

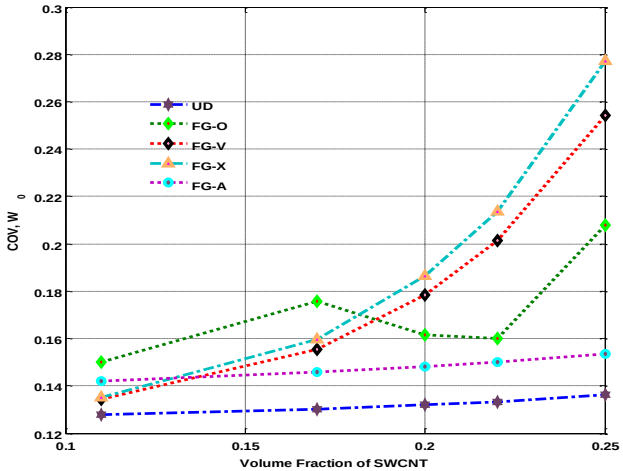

Fig. 14 Effect of random change in all input parameters taken at a time *with* COC=0.1 and different SWCNT volume fraction of various SWCNT-FG plates on CFCF support condition

of deflection of SWCNTRC plate under lateral pressure with (V_{CNT}=0.1 to 0.25, a=b=1, a/h=30, CCCC). The result shows that the COV, W_0 of the FG-O plate is highest, while COV, W_0 of FG-X and FG-V plate are comparatively lowest. Reinforcement of SWCNT in FG-O plate is rich at neutral plane, while in FG-X and FG-V, SWCNT is rich at the top surface of the plate. Hence, FG-O plate is more sensitive as compared to other types of plate. Fig. 8 presents the effect of random change in all random variables b_i, [{(i=1-7)}=0.1] with different configuration of SWCNT on COV of deflection of SWCNTRC plate under lateral pressure with (V_{CNT}=0.17, a=b=1, a/h=20 to100). The result shows that the COV, W0 of the Armchair (5, 5) plate is more than the Armchair (20, 20). It is also observed that COV, W_0 of Armchair (10, 10) and Armchair (15, 15) is lies between armchair (5, 5) and armchair (20,20). Fig. 9 shows the effect of random change in all random variables b_i, [{(i=1-7)}=0.1] with different configuration of SWCNT on COV of deflection of SWCNTRC plate under lateral pressure with (V_{CNT}=0.1 to 0.25, a=b=1, a/h=20, CCCC). The result shows that the COV, W_0 of the Armchair (5, 5) plate is more sensitive than other plates. Fig. 10 depicts the effect random change in all random variables b_i, [{(i=1-7)}=0.1] with different configuration of SWCNT on COV of deflection of SWCNTRC plate under lateral pressure with (V_{CNT}=0.1 to 0.25, a=b=1, a/h=50, SSSS). The result shows that the COV, W_0 of the Armchair (5, 5) plate is more while COV, W_0 armchair (20, 20) plate is low. The COV of defection of armaichai (10, 10) and armachair (15, 15) is lies between armchair (5, 5) and armairch (20, 20). Fig. 11 presents the effect random change in all random variables b_i, [{(i=1-7)}=0.1] with functionally grading (FG) of SWCNT on COV of deflection of SWCNTRC plate under lateral pressure with (V_{CNT}=0.1 to 0.25, a=b=1, a/h=20 to 100, CFCF). It can be seen that increases COV of deflection of SWCNTRC plate with increase in a/h ratio. Hence, the plate is more sensitive when increasing a/h ratio. Fig. 12 shows the effect random change in all random variables b_i, [{(i=1-7)}=0.1] with functionally grading (FG) of SWCNT on COV of deflection of SWCNTRC plate under lateral pressure with (V_{CNT}=0.17, a=b=1, a/h=20 to 10, SSSS). The result shows that the COV, W_0 of the FG-O plate is increased with increase in a/h. Therefore FG-O plate is weaker as compared to other type of plate. Fig. 13 presents the random change in all random variables b_i, [{(i=1-7)}=0.1] with functionally grading (FG) of SWCNT on COV of deflection of SWCNTRC plate under lateral pressure with (V_{CNT}=0.1 to 0.25, a=b=1, a/h=20 to 10, CFCF). The result shows that the COV of deflection of SECNTRC plate decease with increase the volume fraction of CNT. Therefor increase the fibre reinforced in composite then structure is very high strength. Fig. 14 shows the effect random change in all random variables b_i, [{(i=1-7)}=0.1] with functionally grading (FG) of SWCNT on COV of deflection of SWCNTRC plate under lateral pressure with (V_{CNT}=0.1 to 0.25, a=b=1, a/h=75, CFCF). The result shows that the COV, W0 of the FG-X plate is increases with increase in volume fraction of SWCNTs.

One of the most commonly used distributions in engineering problem is normal or Gaussian distribution (Probability Density Function). It is denoted by N (Mean,

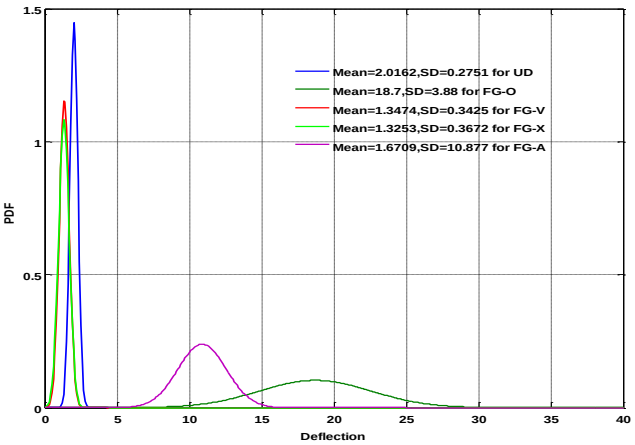

Fig. 15 Normal or Gaussian distribution curves for SWCNTRC-UD and FG plates

standard deviation), indicating that it is a normal random variable with a mean and standard deviation. It considers common in literature the value of a random variable as belonging to a range bounded by the mean plus / minus standard deviation value. For the normal distribution, $Mean \pm 3SD$ bound are established. The deflection range limit is upper and lower bound, they will give a probability of 0.997. Fig. 15 shows the effect of random change in all random variables b_i, [{(i=1-7)}=0.1] with functionally grading (FG) of SWCNT on of probability density function (PDF) of deflection of SWCNTRC plate under lateral pressure with a/h=100 and CCCC supports condition. The result shows that the displacement, lower and upper limit are 1.1909 to 2.8415 for UD plate, thus considering the physical aspect of the parameter, value of displacement between 1.1909 and 2.8415 will effectively give a practical limit to the bounds and will include about 99.7%. The result shows that the desired displacement range is 7.06 to 30.34 for FG-O plate and 99.7% probability. The result shows that the displacement, lower and upper limit are 0.3199 to 2.3749 for FG-V plate, will include about 99.7%. The result shows that the desired displacement ranges are 0.2237 to 2.4269 for FG-X plate; effectively give a practical limit to the bounds and 99.7% probability. The result shows that the desired displacement range is 5.8643 to 15.8897 for FG-A plate, effectively give a practical limit to the bounds and 99.7% probability.

5. Conclusion

A C^0 stochastic finite element method (SFEM) procedure proposed by the present authors in the earlier work is extended by utilizing the existing technique to compute the mean and COV of transverse central deflection of the SWCNTR composite plate in the basis of HSDT with randomness in material properties, plate thickness and uniform transvers loading. The SWCNTRC plate is composed of perfectly bonded SWCNT-FG plate. The presents study, SWCNT are assumed to be uniformly distributed or functionally graded in the thickness direction. The effective material properties of SWCNTRC plates are estimated by micromechanics approach. The numerical results for different grading of SWCNTs, stiffness, shear deformation; volume fraction, boundary condition and chiral index have been presented which shows the effectiveness of the present formulation. The effects of the mean value of UDL load random variables varying simultaneously, width-to-thickness ratio (a/h), boundary condition and volume fraction of SWCNT, different types of SWCNT configuration have been examined in the analysis.

The following conclusions are noted from this study:

- Random system parameter has a dominant effect on the COV of the transverse deflection SWCNTRC plate.
- The COV of the transverse central deflection increases with increase in width-to-thickness ratio and
- The COV of the transverse central deflection decrease with increase in volume fraction of SWCNT.
- The COV of the transverse central deflection of chiral index armchair (5, 5) plate is maximum as compare to other chiral index of SWCNTRC plate.
- The simply supported boundary condition of plate is more sensitive as compared to CCCC, SFSF and CSCS boundary condition.

References

Bounouara, F., Benrahou, K.H., Belkorissat, I. and Tounsi, A. (2016), "A nonlocal zeroth-order shear deformation theory for free vibration of functionally graded nanoscale plates resting on elastic foundation", *Steel Compos. Struct.*, **20**(2), 227-249.

Chakraborty, S., Mandal, B., Chowdhury, R. and Chakrabarti, A. (2016), "Stochastic free vibration analysis of laminated composite plates using polynomial correlated function expansion", *Compos. Struct.*, **135**, 236-249.

Chang, T.P. (2014), "Stochastic dynamic finite element analysis of bridge-vehicle system subjected to random material properties and loadings", *Appl. Math. Comput.*, **242**, 20-35.

Chavan, S.G. and Lal, A. (2017), "Bending behavior of SWCNT reinforced composite plates", *Steel Compos. Struct.*, **24**(5), 537-548.

Chavan, S.G. and Lal, A. (2017), "Bending analysis of laminated SWCNT reinforced functionally graded plate using FEM", *Curv. Layer. Struct.*, **4**(1), 134-145.

Chavan, S.G. and Lal, A. (2017), "Dynamic bending response of SWCNT reinforced composite plates subjected to hygro-thermo-mechanical loading", *Comput. Concrete*, **20**(2), 229-246.

Dey, S., Naskar, S., Mukhopadhyay, T., Gohs, U., Spickenheuer, A., Bittrich, L., ... and Heinrich, G. (2016), "Uncertain natural frequency analysis of composite plates including effect of noise - A polynomial neural network approach", *Compos. Struct.*, **143**, 130-142.

Gadade, A.M., Lal, A. and Singh, B.N. (2016), "Accrate stochastic initial and final faluer of laminated plate subjected to hygrothermo-mechanical loadings using of puck's failure criteria", *Int. J. Mech. Sci.*, **114**, 177-206.

Gadade, A.M., Lal, A. and Singh, B.N. (2016), "Finite element implementation of Puck's failure criterion for failure analysis of laminated plate subjected to biaxial loadings", *Aerosp. Sci. Technol.*, **55**, 227-241.

Gadade, A.M., Lal, A. and Singh, B.N. (2016), "Stochastic progressive failure analysis of laminated composite plates using

Puck's failure criteria", *Mech. Adv. Mater. Struct.*, **23**(7), 739-757.
Kundu, A., DiazDelaO, F.A., Adhikari, S. and Friswell, M.I. (2014), "A hybrid spectral and metamodeling approach for the stochastic finite element analysis of structural dynamic systems", *Comput. Meth. Appl. Mech. Eng.*, **270**, 201-219.
Kwon, Y.W. and Bang, H. (2011), *The Finite Element Method Using MATLAB*, 2ed Edition, CRC Press, New York.
Lal, A. and Singh, B.N. (2009), "Stochastic nonlinear free vibration of laminated composite plates resting on elastic foundation in thermal environments", *Comput. Mech.*, **44**(1), 15-29.
Lal, A. and Singh, B.N. (2010), "Stochastic free vibration of laminated composite plates in thermal environments", *J. Thermoplas. Compos. Mater.*, **23**(1), 57-77.
Lal, A. and Singh, B.N. (2011), "Effect of random system properties on bending response of thermo-mechanically loaded laminated composite plates", *Appl. Math. Model.*, **35**, 5618-5635.
Lal, A., Singh, B.N. and Kale, S. (2011), "Stochastic post buckling analysis of laminated composite cylindrical shell panel subjected to hygro thermomechanical loading", *Compos. Struct.*, **93**, 1187-1200.
Lal, A., Singh, B.N. and Kumar, R. (2007), "Natural frequency of laminated composite plate resting on an elastic foundation with uncertain system properties", *Struct. Eng. Mech.*, **27**(2), 198-222.
Lal, A., Singh, B.N. and Kumar, R. (2008), "Effect of random system properties on initial buckling of composite plates resting on elastic foundation", *Int. J. Struct. Stab. Dyn.*, **8**(1), 103-130.
Lal, A., Singh, B.N. and Patel, D. (2012), "Stochastic nonlinear failure analysis of laminated composite plates under compressive transverse loading", *Compos. Struct.*, **94**, 1211-1223.
Lei, Z. and Qiu, C. (2000), "Neumann dynamic stochastic finite element method of vibration for structures with stochastic parameters to random excitation", *Compos. Struct.*, 77, 651-657.
Li, J., Wu, G., Shen, R. and Hua, H. (2005), "Stochastic bending-torsion coupled response of axially loaded slender composite-thin-walled beams with closed cross-sections", *Int. J. Mech. Sci.*, **47**, 134-155.
Onkar, A.K., Upadhyay, C.S. and Yadav, D. (2007), "Probabilistic failure of laminated composite plates using the stochastic finite element method", *Compos. Struct.*, **77**, 79-91.
Pandit, M.K., Singh, B.N. and Sheikh, A.H. (2009), "Stochastic perturbation-based finite element for deflection statistics of soft core sandwich plate with random material properties", *Int. J. Mech. Sci.*, **51**, 363-371.
Rahmzadeh, A., Ghassemieh, M., Park, Y. and Abolmaali, A. (2016), "Effect of stiffeners on steel plate shear wall systems", *Steel Compos. Struct.*, **20**(3), 545-569.
Sasikumar, P., Suresh, R. and Gupta, S. (2015), "Stochastic model order reduction in uncertainty quantification of composite structures", *Compos. Struct.*, **128**, 21-34.
Sepahvand, K. (2016), "Spectral stochastic finite element vibration analysis of fiber-reinforced composites with random fiber orientation", *Compos. Struct.*, **145**, 119-128.
Shegokar, N.L. and Lal, A. (2013), "Stochastic nonlinear bending response of piezoelectric functionally graded beam subjected to thermoelectromechanical loadings with random material properties", *Compos. Struct.*, **100**, 17-33.
Shi, D.L., Feng, X.Q., Huang, Y.Y., Hwang, K.C. and Gao, H. (2004), "The effect of nanotube waviness and agglomeration on the elastic property of carbon nanotube reinforced composites", *J. Eng. Mater. Technol.*, **126**(3), 250-257.
Singh, B.N. and Lal, A. (2010), "Stochastic analysis of laminated composite plates on elastic foundation: The cases of post-buckling behavior and nonlinear free vibration", *Int. J. Press. Ves. Pip.*, **87**, 559-574.
Singh, B.N. and Lal, A. (2010), "Stochastic analysis of laminated composite plates on elastic foundation: The cases of post-buckling behavior and nonlinear free vibration", *Int. J. Press. Ves. Pip.*, **87**(10), 559-574.
Singh, B.N., Bisht, A.K.S., Pandit, M.K. and Shukla, K.K. (2009), "Nonlinear free vibration analysis of composite plates with material uncertainties: A Monte Carlo simulation approach", *J. Sound Vib.*, **324**, 126-138.
Singh, B.N., Iyengar, N.G.R. and Yadav, D. (2001), "Effects of random material properties on buckling of composite plates", *J. Eng. Mech.*, **127**(9), 873-879.
Singh, B.N., Lal, A. and Kumar, R. (2009), "Post buckling response of laminated composite plate on elastic foundation with random system properties", *Commun. Nonlin. Sci. Numer. Simul.*, **14**, 284-300.
Singh, B.N., Umrao, A., Shukla, K.K. and Vyas, N. (2008), "Second-order statistics of natural frequencies of smart laminated composite plates with random material properties", *Smart Struct. Syst.*, **4**(1), 19-34.
Singh, B.N., Vyas, N. and Dash, P. (2009), "Stochastic free vibration analysis of smart random composite plates", *Struct. Eng. Mech.*, **31**(5), 481-506.
Singh, B.N., Yadav, D. and Iyengar, N.G.R. (2001), "Natural frequencies of composite plates with random material properties using higher-order shear deformation theory", *Int. J. Mech. Sci.*, **43**, 2193-2214.
Singh, B.N., Yadav, D. and Iyengar, N.G.R. (2001), "Stability analysis of laminated cylindrical panels with uncertain material properties", *Compos. Struct.*, **54**, 17-26.
Talha, M. and Singh, B.N. (2014), "Stochastic perturbation-based finite element for buckling statistics of FGM plates with uncertain material properties in thermal environments", *Compos. Struct.*, **108**, 823-833.
Talha, M. and Singh, B.N. (2015), "Stochastic vibration characteristics of finite element modeled functionally gradient plates", *Compos. Struct.*, **130**, 95-106.
Zhang, L.W. and Liew, K.M. (2015), "Large deflection analysis of FG-CNT reinforced Skew plates resting Pasternak foundations using an element-free approach", *Compos. Struct.*, **132**, 974-983.

CC

Nomenclature

E_{11}, E_{22} and E_{33}	=	Young's modulus of the composite plate
ν_{12}, ν_{21}	=	Poison's ratio of composite material
$E_{11}^{CNT}, E_{22}^{CNT} = E_{33}^{CNT}$	=	Young's modulus of CNTs
$G_{12}^{CNT}, G_{23}^{CNT}$ *and* $\nu_{12}^{CNT}, \nu_{21}^{CNT}, \nu_{23}^{CNT}$	=	Shear modulus and poison's ratio of SWCNTs
V^*	=	Total volume fraction of CNT
V_{CNT} and V_m	=	Effective volume fraction of SWCNT and matrix
W_{CNT}, ρ_{CNT} and ρ_m	=	Mass fraction, Density of SWCNT and density of matrix
k_{CNT}, l_{CNT}, n_{CNT}, m_{CNT}	=	Hill elastic constant of

and p_{CNT}		SWCNT
a, b, h	=	Plate length, width and thickness
b_i	=	Basic random material properties
W_0	=	Non-dimensional central deflection
COC	=	Coefficient of Correlation
FGM	=	Functionally graded materials
HSDT	=	Higher Order Shear Deformation Theory
COV	=	Coefficient of Variance
SWCNT	=	Single Wall Carbon Nanotube
SWCNTRC	=	Single Wall Carbon Nanotube Reinforced Composite
UD , FG-O,FG-V,FG-X and FG-A	=	Uniformly Distribution of SWCNT, Types of functionally graded SWCNT
ZOPT	=	Zero Order Perturbation Technique
FOPT	=	First Order Perturbation Technique
SOPT	=	Second Order Perturbation Technique

Appendix

a) The random $[D^R]^l$ matrix terms are expanded.

$$\left[A_4^R\right]=[0]_{3\times4};\left[B_4^R\right]=[0]_{3\times4}$$

$$\left[E_1^R\right]=\left[E_2^R\right]=\left[E_3^R\right]=[0]_{4\times3};\left[C_1^R\right]=\left[A_3^R\right];$$

$$\left[C_2^R\right]=\left[B_3^R\right];\left[C_4^R\right]=[0]_{3\times4}.$$

$$\left[A_1^R\right]=\begin{bmatrix}\int_{-h/2}^{h/2}\frac{Q_{11}}{b_i^R}dz & \int_{-h/2}^{h/2}\frac{Q_{12}}{b_i^R}dz & \int_{-h/2}^{h/2}\frac{Q_{16}}{b_i^R}dz\\ \int_{-h/2}^{h/2}\frac{Q_{12}}{b_i^R}dz & \int_{-h/2}^{h/2}\frac{Q_{22}}{b_i^R}dz & \int_{-h/2}^{h/2}\frac{Q_{26}}{b_i^R}dz\\ \int_{-h/2}^{h/2}\frac{Q_{16}}{b_i^R}dz & \int_{-h/2}^{h/2}\frac{Q_{26}}{b_i^R}dz & \int_{-h/2}^{h/2}\frac{Q_{66}}{b_i^R}dz\end{bmatrix};$$

$$\left[A_2^R\right]=\begin{bmatrix}\int_{-h/2}^{h/2}\frac{Q_{11}}{b_i^R}zdz & \int_{-h/2}^{h/2}\frac{Q_{12}}{b_i^R}zdz & \int_{-h/2}^{h/2}\frac{Q_{16}}{b_i^R}zdz\\ \int_{-h/2}^{h/2}\frac{Q_{12}}{b_i^R}zdz & \int_{-h/2}^{h/2}\frac{Q_{22}}{b_i^R}zdz & \int_{-h/2}^{h/2}\frac{Q_{26}}{b_i^R}zdz\\ \int_{-h/2}^{h/2}\frac{Q_{16}}{b_i^R}zdz & \int_{-h/2}^{h/2}\frac{Q_{26}}{b_i^R}zdz & \int_{-h/2}^{h/2}\frac{Q_{66}}{b_i^R}zdz\end{bmatrix}$$

$$\left[A_3^R\right]=\begin{bmatrix}\int_{-h/2}^{h/2}\frac{Q_{11}}{b_i^R}z^3dz & \int_{-h/2}^{h/2}\frac{Q_{12}}{b_i^R}z^3dz & \int_{-h/2}^{h/2}\frac{Q_{16}}{b_i^R}z^3dz\\ \int_{-h/2}^{h/2}\frac{Q_{12}}{b_i^R}z^3dz & \int_{-h/2}^{h/2}\frac{Q_{22}}{b_i^R}z^3dz & \int_{-h/2}^{h/2}\frac{Q_{26}}{b_i^R}z^3dz\\ \int_{-h/2}^{h/2}\frac{Q_{16}}{b_i^R}z^3dz & \int_{-h/2}^{h/2}\frac{Q_{26}}{b_i^R}z^3dz & \int_{-h/2}^{h/2}\frac{Q_{66}}{b_i^R}z^3dz\end{bmatrix};$$

$$\left[B_1^R\right]=\begin{bmatrix}\int_{-h/2}^{h/2}\frac{Q_{11}}{b_i^R}zdz & \int_{-h/2}^{h/2}\frac{Q_{12}}{b_i^R}zdz & \int_{-h/2}^{h/2}\frac{Q_{16}}{b_i^R}zdz\\ \int_{-h/2}^{h/2}\frac{Q_{12}}{b_i^R}zdz & \int_{-h/2}^{h/2}\frac{Q_{22}}{b_i^R}zdz & \int_{-h/2}^{h/2}\frac{Q_{26}}{b_i^R}zdz\\ \int_{-h/2}^{h/2}\frac{Q_{16}}{b_i^R}zdz & \int_{-h/2}^{h/2}\frac{Q_{26}}{b_i^R}zdz & \int_{-h/2}^{h/2}\frac{Q_{66}}{b_i^R}zdz\end{bmatrix};$$

$$\left[B_2^R\right]=\begin{bmatrix}\int_{-h/2}^{h/2}\frac{Q_{11}}{b_i^R}z^2dz & \int_{-h/2}^{h/2}\frac{Q_{12}}{b_i^R}z^2dz & \int_{-h/2}^{h/2}\frac{Q_{16}}{b_i^R}z^2dz\\ \int_{-h/2}^{h/2}\frac{Q_{12}}{b_i^R}z^2dz & \int_{-h/2}^{h/2}\frac{Q_{22}}{b_i^R}z^2dz & \int_{-h/2}^{h/2}\frac{Q_{26}}{b_i^R}z^2dz\\ \int_{-h/2}^{h/2}\frac{Q_{16}}{b_i^R}z^2dz & \int_{-h/2}^{h/2}\frac{Q_{26}}{b_i^R}z^2dz & \int_{-h/2}^{h/2}\frac{Q_{66}}{b_i^R}z^2dz\end{bmatrix}$$

$$\left[B_3^R\right]=\begin{bmatrix}\int_{-h/2}^{h/2}\frac{Q_{11}}{b_i^R}z^4dz & \int_{-h/2}^{h/2}\frac{Q_{12}}{b_i^R}z^4dz & \int_{-h/2}^{h/2}\frac{Q_{16}}{b_i^R}z^4dz\\ \int_{-h/2}^{h/2}\frac{Q_{12}}{b_i^R}z^4dz & \int_{-h/2}^{h/2}\frac{Q_{22}}{b_i^R}z^4dz & \int_{-h/2}^{h/2}\frac{Q_{26}}{b_i^R}z^4dz\\ \int_{-h/2}^{h/2}\frac{Q_{16}}{b_i^R}z^4dz & \int_{-h/2}^{h/2}\frac{Q_{26}}{b_i^R}z^4dz & \int_{-h/2}^{h/2}\frac{Q_{66}}{b_i^R}z^4dz\end{bmatrix};$$

$$\left[C_3^R\right]=\begin{bmatrix}\int_{-h/2}^{h/2}\frac{Q_{11}}{b_i^R}z^6dz & \int_{-h/2}^{h/2}\frac{Q_{12}}{b_i^R}z^6dz & \int_{-h/2}^{h/2}\frac{Q_{16}}{b_i^R}z^6dz\\ \int_{-h/2}^{h/2}\frac{Q_{12}}{b_i^R}z^6dz & \int_{-h/2}^{h/2}\frac{Q_{22}}{b_i^R}z^6dz & \int_{-h/2}^{h/2}\frac{Q_{26}}{b_i^R}z^6dz\\ \int_{-h/2}^{h/2}\frac{Q_{16}}{b_i^R}z^6dz & \int_{-h/2}^{h/2}\frac{Q_{26}}{b_i^R}z^6dz & \int_{-h/2}^{h/2}\frac{Q_{66}}{b_i^R}z^6dz\end{bmatrix}$$

$$\left[E_4^R\right]=\begin{bmatrix}\int_{-h/2}^{h/2}\frac{Q_{44}}{b_i^R}dz & \int_{-h/2}^{h/2}\frac{Q_{45}}{b_i^R}dz & \int_{-h/2}^{h/2}\frac{Q_{44}}{b_i^R}z^2dz & \int_{-h/2}^{h/2}\frac{Q_{45}}{b_i^R}z^2dz\\ \int_{-h/2}^{h/2}\frac{Q_{45}}{b_i^R}dz & \int_{-h/2}^{h/2}\frac{Q_{55}}{b_i^R}dz & \int_{-h/2}^{h/2}\frac{Q_{45}}{b_i^R}z^2dz & \int_{-h/2}^{h/2}\frac{Q_{55}}{b_i^R}z^2dz\\ \int_{-h/2}^{h/2}\frac{Q_{44}}{b_i^R}z^2dz & \int_{-h/2}^{h/2}\frac{Q_{45}}{b_i^R}z^2dz & \int_{-h/2}^{h/2}\frac{Q_{44}}{b_i^R}z^4dz & \int_{-h/2}^{h/2}\frac{Q_{45}}{b_i^R}z^4dz\\ \int_{-h/2}^{h/2}\frac{Q_{45}}{b_i^R}z^2dz & \int_{-h/2}^{h/2}\frac{Q_{55}}{b_i^R}z^2dz & \int_{-h/2}^{h/2}\frac{Q_{45}}{b_i^R}z^4dz & \int_{-h/2}^{h/2}\frac{Q_{55}}{b_i^R}z^5dz\end{bmatrix}$$

b) The random $[D^R]^{II}$ matrix terms are expanded,

$$\left[B_{21}^R\right]=\left[A_{12}^R\right];\left[C_{31}^R\right]=\left[A_{13}^R\right];\left[C_{32}^R\right]=\left[B_{23}^R\right];$$

$$\left[E_{41}^R\right]=\left[E_{42}^R\right]=\left[E_{43}^R\right]=\left[0\right]_{4\times3};$$

$$\left[A_{14}^R\right]=\left[A_{24}^R\right]=\left[A_{34}^R\right]=\left[0\right]_{3\times4}.$$

$$\left[A_{11}^R\right]=\begin{bmatrix}\int_{-h/2}^{h/2}\frac{Q_{11}}{2\left(b_i^R\right)^2}dz & \int_{-h/2}^{h/2}\frac{Q_{12}}{2\left(b_i^R\right)^2}dz & \int_{-h/2}^{h/2}\frac{Q_{16}}{2\left(b_i^R\right)^2}dz\\ \int_{-h/2}^{h/2}\frac{Q_{12}}{2\left(b_i^R\right)^2}dz & \int_{-h/2}^{h/2}\frac{Q_{22}}{2\left(b_i^R\right)^2}dz & \int_{-h/2}^{h/2}\frac{Q_{26}}{2\left(b_i^R\right)^2}dz\\ \int_{-h/2}^{h/2}\frac{Q_{16}}{2\left(b_i^R\right)^2}dz & \int_{-h/2}^{h/2}\frac{Q_{26}}{2\left(b_i^R\right)^2}dz & \int_{-h/2}^{h/2}\frac{Q_{66}}{2\left(b_i^R\right)^2}dz\end{bmatrix}$$

$$\left[A_{12}^R\right]=\begin{bmatrix}\int_{-h/2}^{h/2}\frac{Q_{11}}{2\left(b_i^R\right)^2}zdz & \int_{-h/2}^{h/2}\frac{Q_{12}}{2\left(b_i^R\right)^2}zdz & \int_{-h/2}^{h/2}\frac{Q_{16}}{2\left(b_i^R\right)^2}zdz\\ \int_{-h/2}^{h/2}\frac{Q_{12}}{2\left(b_i^R\right)^2}zdz & \int_{-h/2}^{h/2}\frac{Q_{22}}{2\left(b_i^R\right)^2}zdz & \int_{-h/2}^{h/2}\frac{Q_{26}}{2\left(b_i^R\right)^2}zdz\\ \int_{-h/2}^{h/2}\frac{Q_{16}}{2\left(b_i^R\right)^2}zdz & \int_{-h/2}^{h/2}\frac{Q_{26}}{2\left(b_i^R\right)^2}zdz & \int_{-h/2}^{h/2}\frac{Q_{66}}{2\left(b_i^R\right)^2}zdz\end{bmatrix}$$

$$\left[A_{13}^R\right]=\begin{bmatrix}\int_{-h/2}^{h/2}\frac{Q_{11}}{2\left(b_i^R\right)^2}z^3dz & \int_{-h/2}^{h/2}\frac{Q_{12}}{2\left(b_i^R\right)^2}z^3dz & \int_{-h/2}^{h/2}\frac{Q_{16}}{2\left(b_i^R\right)^2}z^3dz\\ \int_{-h/2}^{h/2}\frac{Q_{12}}{2\left(b_i^R\right)^2}z^3dz & \int_{-h/2}^{h/2}\frac{Q_{22}}{2\left(b_i^R\right)^2}z^3dz & \int_{-h/2}^{h/2}\frac{Q_{26}}{2\left(b_i^R\right)^2}z^3dz\\ \int_{-h/2}^{h/2}\frac{Q_{16}}{2\left(b_i^R\right)^2}z^3dz & \int_{-h/2}^{h/2}\frac{Q_{26}}{2\left(b_i^R\right)^2}z^3dz & \int_{-h/2}^{h/2}\frac{Q_{66}}{2\left(b_i^R\right)^2}z^3dz\end{bmatrix}$$

$$\left[B_{22}^R\right]=\begin{bmatrix}\int_{-h/2}^{h/2}\frac{Q_{11}}{2\left(b_i^R\right)^2}z^2dz & \int_{-h/2}^{h/2}\frac{Q_{12}}{2\left(b_i^R\right)^2}z^2dz & \int_{-h/2}^{h/2}\frac{Q_{16}}{2\left(b_i^R\right)^2}z^2dz\\ \int_{-h/2}^{h/2}\frac{Q_{12}}{2\left(b_i^R\right)^2}z^2dz & \int_{-h/2}^{h/2}\frac{Q_{22}}{2\left(b_i^R\right)^2}z^2dz & \int_{-h/2}^{h/2}\frac{Q_{26}}{2\left(b_i^R\right)^2}z^2dz\\ \int_{-h/2}^{h/2}\frac{Q_{16}}{2\left(b_i^R\right)^2}z^2dz & \int_{-h/2}^{h/2}\frac{Q_{26}}{2\left(b_i^R\right)^2}z^2dz & \int_{-h/2}^{h/2}\frac{Q_{66}}{2\left(b_i^R\right)^2}z^2dz\end{bmatrix}$$

$$\left[B_{23}^R\right]=\begin{bmatrix}\int_{-h/2}^{h/2}\frac{Q_{11}}{2\left(b_i^R\right)^2}z^4dz & \int_{-h/2}^{h/2}\frac{Q_{12}}{2\left(b_i^R\right)^2}z^4dz & \int_{-h/2}^{h/2}\frac{Q_{16}}{2\left(b_i^R\right)^2}z^4dz\\ \int_{-h/2}^{h/2}\frac{Q_{12}}{2\left(b_i^R\right)^2}z^4dz & \int_{-h/2}^{h/2}\frac{Q_{22}}{2\left(b_i^R\right)^2}z^4dz & \int_{-h/2}^{h/2}\frac{Q_{26}}{2\left(b_i^R\right)^2}z^4dz\\ \int_{-h/2}^{h/2}\frac{Q_{16}}{2\left(b_i^R\right)^2}z^4dz & \int_{-h/2}^{h/2}\frac{Q_{26}}{2\left(b_i^R\right)^2}z^4dz & \int_{-h/2}^{h/2}\frac{Q_{66}}{2\left(b_i^R\right)^2}z^4dz\end{bmatrix}$$

$$\left[C_{33}^R\right]=\begin{bmatrix}\int_{-h/2}^{h/2}\frac{Q_{11}}{2\left(b_i^R\right)^2}z^6dz & \int_{-h/2}^{h/2}\frac{Q_{12}}{2\left(b_i^R\right)^2}z^6dz & \int_{-h/2}^{h/2}\frac{Q_{16}}{2\left(b_i^R\right)^2}z^6dz\\ \int_{-h/2}^{h/2}\frac{Q_{12}}{2\left(b_i^R\right)^2}z^6dz & \int_{-h/2}^{h/2}\frac{Q_{22}}{2\left(b_i^R\right)^2}z^6dz & \int_{-h/2}^{h/2}\frac{Q_{26}}{2\left(b_i^R\right)^2}z^6dz\\ \int_{-h/2}^{h/2}\frac{Q_{16}}{2\left(b_i^R\right)^2}z^6dz & \int_{-h/2}^{h/2}\frac{Q_{26}}{2\left(b_i^R\right)^2}z^6dz & \int_{-h/2}^{h/2}\frac{Q_{66}}{2\left(b_i^R\right)^2}z^6dz\end{bmatrix}$$

$$\left[E_{44}^R\right]=\begin{bmatrix}\int_{-h/2}^{h/2}\frac{Q_{44}}{2\left(b_i^R\right)^2}dz & \int_{-h/2}^{h/2}\frac{Q_{45}}{2\left(b_i^R\right)^2}dz & \int_{-h/2}^{h/2}\frac{Q_{44}}{2\left(b_i^R\right)^2}z^2dz & \int_{-h/2}^{h/2}\frac{Q_{45}}{2\left(b_i^R\right)^2}z^2dz\\ \int_{-h/2}^{h/2}\frac{Q_{45}}{2\left(b_i^R\right)^2}dz & \int_{-h/2}^{h/2}\frac{Q_{55}}{2\left(b_i^R\right)^2}dz & \int_{-h/2}^{h/2}\frac{Q_{45}}{2\left(b_i^R\right)^2}z^2dz & \int_{-h/2}^{h/2}\frac{Q_{55}}{2\left(b_i^R\right)^2}z^2dz\\ \int_{-h/2}^{h/2}\frac{Q_{44}}{2\left(b_i^R\right)^2}z^2dz & \int_{-h/2}^{h/2}\frac{Q_{45}}{2\left(b_i^R\right)^2}z^2dz & \int_{-h/2}^{h/2}\frac{Q_{44}}{2\left(b_i^R\right)^2}z^4dz & \int_{-h/2}^{h/2}\frac{Q_{45}}{2\left(b_i^R\right)^2}z^4dz\\ \int_{-h/2}^{h/2}\frac{Q_{45}}{2\left(b_i^R\right)^2}z^2dz & \int_{-h/2}^{h/2}\frac{Q_{55}}{2\left(b_i^R\right)^2}z^2dz & \int_{-h/2}^{h/2}\frac{Q_{45}}{2\left(b_i^R\right)^2}z^4dz & \int_{-h/2}^{h/2}\frac{Q_{55}}{2\left(b_i^R\right)^2}z^5dz\end{bmatrix}$$